Thermodynamic properties of classical plasmas in a polarizing background: Numerical experiments

Hiroo Totsuji and Kenji Tokami
Department of Electronics, Okayama University, Tsushimanaka, Okayama 700, Japan
(Received 4 May 1984)

Thermodynamic properties of strongly coupled classical ions in the polarizing background of degenerate electrons are analyzed by numerical experiments. The effect of finite electron temperature is taken into account. The internal energy, the pressure, the pair-correlation function, and the structure factor of ions are obtained, and the effects of electronic screening on these quantities are clarified.

I. INTRODUCTION

Properties of dense ionized matter have been investigated not only because of interest in them as a subject of statistical physics but also because of their importance in applications to liquid metals, molten salts, and dense matter of astrophysical interest, and those related to the inertial confinement fusion by intense laser irradiation.

In most of these dense ionized matter, ions (nuclei) behave classically in the background of degenerate electrons. When we neglect the electronic response to ionic charges, the classical one-component plasma (OCP), the classical system of charged particles in the rigid uniform background, works as a useful model to analyze these matters. The static and dynamic properties of the OCP have been studied by a number of investigators[1] and these results are extensively used in the OCP model of ionized matters. The OCP also provides a useful reference system for the variational or perturbative calculations in the cases where interaction potentials have small deviations from the pure Coulomb potential.

Though the OCP model explains many important characteristics of dense ionized matter, there exists a domain of physical parameters where one has to take into account the polarization of electrons. Ionic charges are screened by the induced charge of electrons and static and dynamic properties of the system are thereby modified from those of the OCP.

Various investigations have been done to analyze the effect of electronic screening. Monte Carlo numerical experiments have been performed[2–4] including the case of ionic mixtures. Their results have been compared with the variational calculations[5,6] based on the knowledge of the hard-sphere system or the OCP.

In the above investigations the response of electrons has been described by the linear response theory and electrons are assumed to be completely degenerate. Thus the zero-temperature values of the random-phase approximation (RPA) by Lindhard[7] have been used as the dielectric response function of electrons.

The framework of the linear response may be applicable in the case of weak electronic screening. The polarizability of electrons, however, depends on the temperature as well as the density. In the case of strong ionic coupling, the temperature is much smaller than the Fermi energy of electrons and the electrons can be regarded as completely degenerate. When the coupling between ions is weak or intermediate, however, the temperature has substantial effect on the polarizability of electrons, and the ratio of the temperature to the Fermi energy of the electrons cannot be neglected even in the case of weak electronic screening.

In addition to the assumption of the complete degeneracy of electrons, the accuracy of the pair-distribution function in previous numerical experiments has not been sufficient to clarify the potential of mean force or the structure factor of ions. These quantities are necessary to calculate the enhancement of the thermonuclear-reaction rate or electronic-transport coefficients. The purpose of this paper is to analyze the effect of electronic screening on thermodynamic quantities and the pair-correlation function of ions by numerical experiments in which the temperature of electrons is taken into account.

II. MODEL AND METHOD OF NUMERICAL EXPERIMENTS

A. Model Hamiltonian

We consider two-component plasmas composed of protons (the number density n_i and the charge e) and electrons (the number density $n_e=n_i$ and the charge $-e$) in thermodynamic equilibrium at the temperature T. Two-component plasmas are characterized by two nondimensional parameters, the parameter Γ of the classical ions and the parameter r_s of the degenerate electrons, defined respectively by

$$\Gamma=e^2/k_BTa\ , \tag{2.1}$$

$$r_s=a_e/a_B\ . \tag{2.2}$$

Here $a=(3/4\pi n_i)^{1/3}$ is the ion-sphere radius, $a_e=(3/4\pi n_e)^{1/3}=a$, a_B is the Bohr radius, and k_B is the Boltzmann constant. The combinations of the parameters in our numerical experiments are shown in Table I.

The ratio τ of the temperature T to the Fermi energy of electrons $E_F=\hbar^2(3\pi^2n_e)^{2/3}/2m_e$ (m_e and $\hbar$ are the elec-

TABLE I. Parameters of numerical experiments.

r_s	Γ	$\tau=k_BT/E_F$	Number of particles	Number of steps (10^5)
1	1	0.543	64	2
	2	0.272	64	2
	5	0.109	128	1
	10	0.0543	128	1
	50	0.0109	250	0.5
0.1	1	0.0543	64	2
	2	0.0272	64	2
	5	0.0109	128	1
	10	0.005 43	128	1
0.01	2	0.005 43	64	2

tronic mass and the Planck's constant) is given by

$$\tau=k_BT/E_F=2(4/9\pi)^{2/3}(r_s/\Gamma)$$
$$=0.543(r_s/\Gamma) \tag{2.3}$$

and is shown in Table I. The value of τ becomes substantial when r_s is large and Γ is small; the maximum 0.543 is attained for $r_s=1$ and $\Gamma=1$ in the parameter range of our experiments.

We restrict ourselves in the domain $r_s\leq 1$ where the response of electrons may be described by the linear-response theory. Due to the large ion-electron mass ratio, the potential due to the electronic charge induced around an ion is given in terms of the static dielectric response function $\epsilon_e(k,\omega=0)$ of electrons. The effective potential $v(r)$ between ions is thus given by

$$v(r)/k_BT=e^2/k_BTr-\Gamma\psi(r)$$
$$=\Gamma[a/r-\psi(r)]\ , \tag{2.4}$$

where

$$\psi(r)=a(2\pi)^{-3}\int d\vec{k}(4\pi/k^2)$$
$$\times[1-1/\epsilon_e(k,0)]\exp(i\vec{k}\cdot\vec{r})\ . \tag{2.5}$$

The interaction energy U is a function of the coordinates $\{\vec{r}_i\}$ of ions and is composed of two parts, $U^{(0)}$ and $U^{(1)}$, as

$$U=U^{(0)}+U^{(1)}\ . \tag{2.6}$$

Here $U^{(0)}$ is the OCP part which comes from the Coulomb interaction e^2/r between ions and $U^{(1)}$ is the ion-electron interaction energy given by

$$U^{(1)}=-(e^2/2a)\sum_{i,j}\psi(r_{ij}) \tag{2.7}$$

with

$$\vec{r}_{ij}=\vec{r}_i-\vec{r}_j\ .$$

The nonideal part of the pressure ΔP of the ion system is given by the derivative (with respect to the volume V) of the Helmholtz free energy related to the ion configuration and is calculated as

$$V\Delta P/k_BT=\langle U\rangle/3k_BT+(\Gamma/2)\left\langle\sum_{i,j}a(2\pi)^{-3}\int d\vec{k}\{4\pi/k^2[\epsilon_e(k,0)]^2\}V(\partial/\partial V)\epsilon_e(k,0)\exp(i\vec{k}\cdot\vec{r}_{ij})\right\rangle\ . \tag{2.8}$$

Here $\langle\ \rangle$ denotes the statistical average and

$$V(\partial/\partial V)\epsilon_e(k,0)=[(r_s/3)(\partial/\partial r_s)+(2\tau/3)(\partial/\partial\tau)]\epsilon_e(k,\omega=0;r_s,\tau)\ . \tag{2.9}$$

B. Dielectric response function of electrons

As for the dielectric response function of electrons, we mainly use the one in the random-phase approximation (RPA) for finite temperatures given by[7]

$$\epsilon_e(k,\omega=0;r_s,\tau)=1+(2/\pi)(4/9\pi)^{1/3}r_s(k/k_F)^{-3}\int_0^\infty dx\,f(x)\ln|(x^{1/2}+k/2k_F)/(x^{1/2}-k/2k_F)| \tag{2.10}$$

with

$$f(x)=\{\exp[(x-\mu')/\tau]+1\}^{-1}\ ,$$
$$\mu'=\mu/E_F\ ,$$

where $k_F=(3\pi^2n_e)^{1/3}$ is the Fermi wave number and μ is the chemical potential. Note that μ' is a function of τ.

For this dielectric response function, the derivatives appearing in (2.9) are calculated as

$$r_s(\partial/\partial r_s)\epsilon_e=\epsilon_e-1\ , \tag{2.11}$$

$$\tau(\partial/\partial\tau)\epsilon_e=(2/\pi)(4/9\pi)^{1/3}(k/k_F)^{-3}\int_0^\infty dx\, f(x)[1-f(x)][(x-\mu')/\tau+(\partial\mu'/\partial\tau)] \times\ln|(x^{1/2}+k/2k_F)/(x^{1/2}-k/2k_F)|\ . \tag{2.12}$$

In Fig. 1 we plot the function $\psi(r)$ in comparison with the Coulomb potential for some values of the parameters. For $r_s=1$, $\psi(r)$ increases with the increase of Γ and approaches the limit of zero temperature which is slightly above the values for $\Gamma=5$. For $r_s=0.1$ and $\Gamma\gtrsim 1$, $\psi(r)$ is almost indistinguishable from the zero-temperature limit.

As is shown in Fig. 1, the finite-temperature effect decreases the electronic screening. This tendency appears also in the long-wavelength asymptote of the dielectric response function for $\tau\ll 1$

$$\epsilon_e(k,\omega=0)=1+(4\pi e^2/k^2)(\partial n_e/\partial\mu)_T,\quad k\ll k_F \tag{2.13}$$

as

$$4\pi e^2(\partial n_e/\partial\mu)_T=k_{\mathrm{FT}}^2[1-(\pi^2/12)\tau^2],\quad \tau\ll 1 \tag{2.14}$$

where $k_{\mathrm{FT}}=(6\pi n_e e^2/E_F)^{1/2}$ is the Fermi-Thomas wave number.

The RPA dielectric response function does not include the local-field correction. In Fig. 2 we show the values of the function $\psi(r)$ for $r_s=1$ at zero temperature calculated by the RPA dielectric response function and those given by the dielectric response functions with local-field corrections due to Hubbard[8] and Ichimaru and Utsumi.[9] Both local-field corrections give almost the same values which are about 4% larger than the RPA values near $r=0$. The local-field correction increases the screening at zero temperature.

As is shown in Figs. 1 and 2, the finiteness of the temperature and the local-field correction at zero temperature have the effects in the opposite directions on the electronic screening. For $r_s=1$ and $\Gamma=1$, the former effect is more than two times larger than the latter. Though it may happen that the local-field correction has a comparable or larger effect than the finiteness of the temperature for large values of Γ, little is known about the local-field correction at finite temperatures. We therefore adopt the RPA dielectric response function in our experiments.

Since the relativistic effect becomes important for small values of r_s, we use the relativistic expression of the RPA dielectric response function due to Jancovici[10] for $r_s=0.01$; the finiteness of the temperature can be neglected in this case.

C. Method of numerical experiments

We impose the periodic boundary conditions of simple-cubic symmetry on our system and evaluate U for the unit cell of volume V_0 containing N_0 independent particles. The Coulomb interactions between particles and their periodic images are evaluated by the Ewald's procedure as

$$U^{(0)}=(e^2/2)\sum_{i\neq j}\sum_{\vec{l}}\mathrm{erfc}(G\,|\,\vec{r}_{ij}-\vec{l}\,|\,)/|\,\vec{r}_{ij}-\vec{l}\,| +(e^2/2V_0)\sum_{\vec{g}\,(\neq\vec{0})}(4\pi/g^2)\exp(-g^2/4G^2)(\rho_{\vec{g}}\rho_{-\vec{g}}-N_0)-[N_0(N_0-1)/2]\pi e^2/G^2V_0+N_0U_0 \tag{2.15}$$

with

$$\rho_{\vec{g}}=\sum_i\exp(-i\vec{g}\cdot\vec{r}_i)$$

and

$$\mathrm{erfc}(x)=(2/\pi^{1/2})\int_x^\infty dt\exp(-t^2)\ .$$

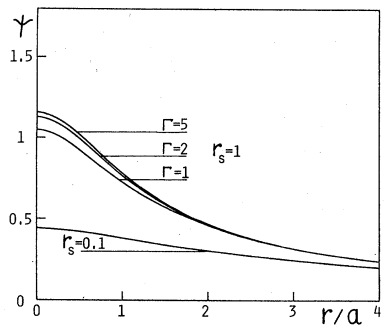

FIG. 1. Screening of ion interaction by electrons $\psi(r)$.

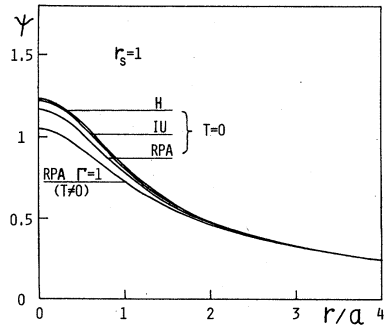

FIG. 2. Effect of zero-temperature local-field correction on $\psi(r)$ in comparison with finite-temperature effect. *H* (Hubbard) and *IU* (Ichimaru and Utsumi) (*H* is slightly above *IU*) curves are calculated with local-field corrections in Refs. 8 and 9, respectively.

Here $\vec{l}$ and $\vec{g}$ belong to the simple-cubic lattice and its reciprocal lattice, respectively; U_0 is the Madelung energy (per particle) of the simple-cubic lattice; G is an arbitrary constant.

Similar lattice sums related to $\psi(r)$ are given by a slowly converging series in the Fourier space. We convert this series into the sum of two rapidly converging ones in real and Fourier spaces: We add and subtract a function which has a simple form in the real space and, at the same time, has the same asymptotic behavior as the original series in the Fourier space. Thus $U^{(1)}$ is rewritten as

$$U^{(1)}=(e^2/2V_0)\sum_{\vec{g}\ (\neq\vec{0})}(4\pi/g^2)\rho_{\vec{g}}\rho_{-\vec{g}}\{[\epsilon_e(g,0)]^{-1}-1+A(r_sk_F^4g^2)(g^2+B^2k_F^2)^{-3}\}$$
$$-A(r_se^2k_F)(16B^3)^{-1}\sum_{i,j}\sum_{\vec{l}}(1+Bk_F\,|\,\vec{r}_{ij}-\vec{l}\,|\,)\exp(-Bk_F\,|\,\vec{r}_{ij}-\vec{l}\,|\,)+AN_0^2(2\pi e^2r_s)/k_F^2V_0B^6\,, \tag{2.16}$$

where $A=(16/3\pi)(4/9\pi)^{1/3}$ and B is an arbitrary constant. The interaction energy per unit cell is given by $\langle U^{(0)}+U^{(1)}\rangle$ and we determine the values of G and B to minimize the computational time.

Thermodynamic equilibrium of our two-component plasma is simulated by the standard Monte Carlo method of Metropolis *et al.*[11] The range of the pair correlation increases with the value of Γ and we need to increase the number of independent particles for larger Γ. For the values of Γ of interest, however, a relatively small number of independent particles may be sufficient. Since much more computational time is needed than the case of simple Coulomb potential, we have to perform experiments with a relatively small number of independent particles. The number of independent particles used in our experiments and the number of Monte Carlo steps (after discarded initial steps) are tabulated in Table I.

III. RESULTS

A. Interaction energy

When the electrons screen ionic charges, the internal energy $\langle U\rangle$ decreases due to negative interaction energy between ions and electrons. The value of the interaction energy is given in Table II and the relative deviation from the OCP value[12] is plotted in Fig. 3. The values obtained by earlier numerical experiments[4] and the results of the variational calculations[5] are also shown in Fig. 3. When $r_s=0.1$, our results are consistent with variational calculations[5] for $\Gamma\geq 2$; earlier experiments give smaller values for $\Gamma\geq 2$.

For $r_s=1$ and $\Gamma\geq 2$, our results are consistent with both variational calculations[5] and earlier experiments.[4] For $r_s=1$ and $\Gamma=1$, the decrease of the interaction energy is smaller, as expected, than earlier numerical experiments[4] which neglected the effect of incomplete degeneracy of electrons: For the same density, screening of electrons becomes weaker with the increase of the temperature.

TABLE II. Interaction energy and pressure. (Values for the OCP are taken from Ref. 12.)

Γ	r_s	$\langle U\rangle/N_0k_BT$	$V\Delta P/N_0k_BT$
1	1	−0.715±0.003	−0.223±0.001
	0.1	−0.599±0.002	−0.189±0.001
	0	−0.572	−0.191
2	1	−1.574±0.001	−0.463±0.002
	0.1	−1.355±0.003	−0.435±0.002
	0.01	−1.336±0.003	−0.441±0.001
	0	−1.320	−0.440
5	1	−4.219±0.001	−1.233±0.003
	0.1	−3.809±0.001	−1.240±0.002
	0	−3.757	−1.252
10	1	−8.746±0.003	−2.608±0.001
	0.1	−8.082±0.007	−2.654±0.005
	0	−7.998	−2.666
50	1	−45.965±0.035	−14.304±0.022
	0	−43.102	−14.367

B. Pressure

The nonideal part of the pressure of the ionic system ΔP is given in Table II and the relative deviation from the OCP value[12] is plotted in Figs. 4(a) and 4(b), where the results of earlier experiments[4] and those of variational calculations[5] are also shown. For $r_s=0.1$ the deviation is

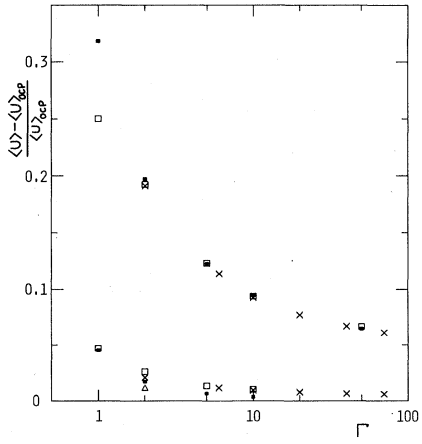

FIG. 3. $(\langle U\rangle-\langle U\rangle_{\rm OCP})/\langle U\rangle_{\rm OCP}$. Present results (open squares) are compared with earlier experiments (dots, Ref. 4) and variational calculations (×, Ref. 5). Upper group is for $r_s=1$ and lower one is for $r_s=0.1$. △ is present result for $r_s=0.01$. Note that $\langle U\rangle_{\rm OCP}$ is negative.

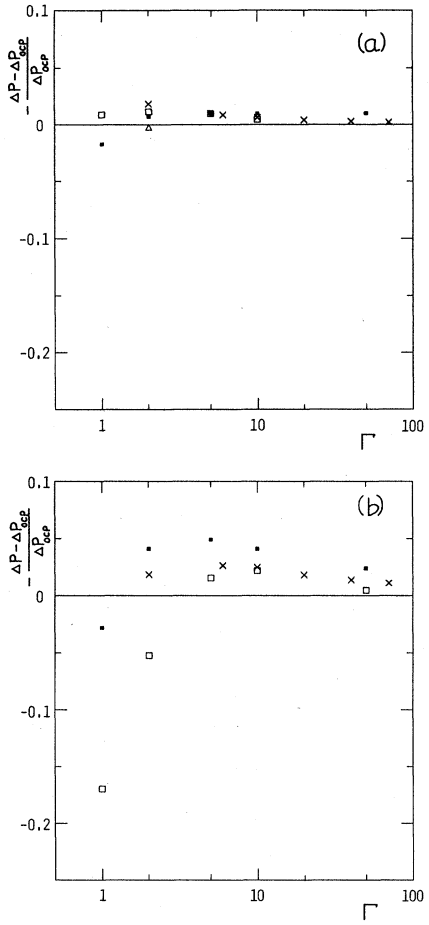

FIG. 4. (a) $-(\Delta P-\Delta P_{\rm OCP})/\Delta P_{\rm OCP}$ for $r_s=0.1$ and 0.01. Symbols are the same as in Fig. 3. Note that $\Delta P_{\rm OCP}$ is negative. (b) The same as (a) for $r_s=1$.

positive and our results are consistent with variational calculations. Our results are also similar to earlier experiments except for small values of Γ.

When $r_s=1$, the deviation is positive for $\Gamma\gtrsim 5$ but is negative for $\Gamma\lesssim 2$. Our results systematically differ from those of earlier experiments, not only for small Γ for which the finite-temperature effect is significant but also for large Γ for which that effect is apparently small. Except for $5\lesssim\Gamma\lesssim 10$, variational calculations give larger values; the difference is most remarkable for $\Gamma\lesssim 2$.

When the density increases, Γ increases and r_s and τ decrease. The increase of Γ decreases the ionic interaction energy and therefore makes a negative contribution to the pressure. The decrease of τ increases the electronic screening and also decreases the pressure. The decrease of r_s, on the other hand, decreases the electronic screening and increases the pressure. The first effect and the second and third effects are expressed by the first and the second terms on the right-hand side of (2.8), respectively. The behavior of the pressure is the result of competition between these effects.

As we see in Fig. 3, the decrease of the interaction energy due to finite-temperature electronic screening for $r_s=1$ and $\Gamma=1$ is smaller than the zero-temperature case; this effect of finite temperature gives a positive contribution to the deviation of pressure through the first term of (2.8). Negative deviations of the pressure for $r_s=1$ and $\Gamma\lesssim 2$ in our experiments indicate that the finiteness of the temperature significantly affects the second term of (2.8) in the negative direction.

It has been known[5,6] that the local-field correction at zero temperature also has a large effect on the deviation of the pressure. Thus the deviation of the pressure of an ionic system is very sensitive to both the finite-temperature effect and the local-field correction in the electronic dielectric response function. Our results without local-field correction may provide a boundary condition to analyze the effect of local-field correction at finite temperature.

C. Pair-correlation function

As is shown in Sec. II, the short-range repulsion between ions is reduced by the screening effect of electrons. The pair-distribution function $g(r)$ therefore increases in the short-range domain. This tendency has already been shown by earlier numerical experiments but the precise values have not been analyzed. We now analyze the behavior of the pair-correlation function in detail.

In Figs. 5(a)–5(e) we show the nonideal part $H(r)$ of the potential of the mean force defined by

$$g(r)=\exp[-e^2/k_BTr+H(r)]=\exp[-\Gamma a/r+H(r)], \tag{3.1}$$

TABLE III. Coefficients of fitting function for $H(r)/\Gamma$.

Γ	r_s	c_0	c_1	c_2	Range of r min.	Range of r max.
1	1	1.487	−0.747	0.127	0.34	1.79
	0.1	1.110	−0.342	0.013	0.31	1.76
2	1	1.630	−0.930	0.188	0.27	1.82
	0.1	1.275	−0.502	0.056	0.56	1.82
5	1	1.634	−0.866	0.148	0.37	1.83
	0.1	1.271	−0.419	0.013	0.49	1.79
10	1	1.677	−0.911	0.161	0.57	1.79
	0.1	1.300	−0.443	0.019	0.73	1.79
50	1	1.572	−0.799	0.133	0.91	1.83

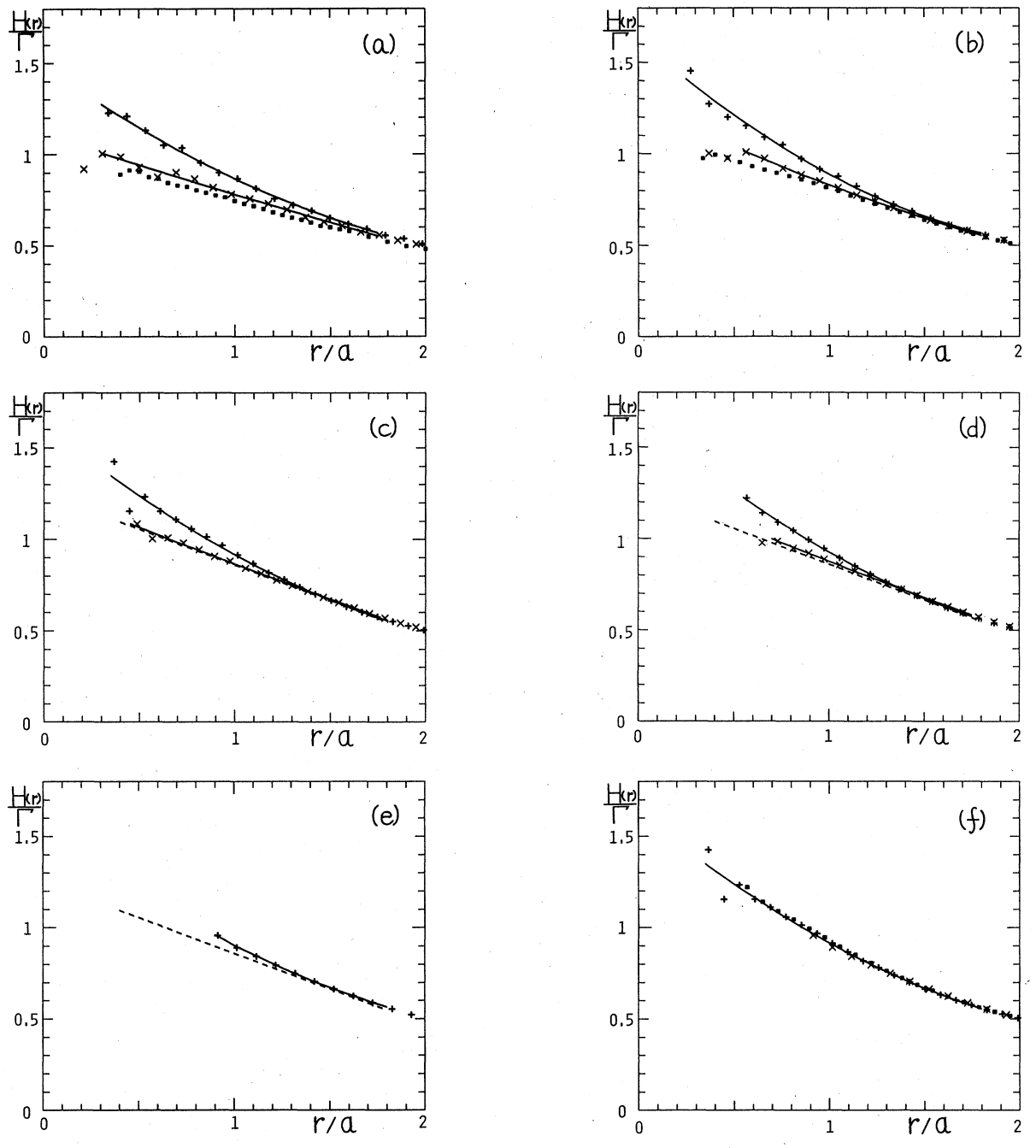

FIG. 5. (a) $H(r)/\Gamma$ for $\Gamma=1$ with $r_s=1$ (+) and 0.1 (×). OCP values (dots) are taken from Ref. 13. Solid lines are interpolations (3.3) with coefficients given in Table III. (b) The same as (a) for $\Gamma=2$. OCP values are taken from Ref. 14. (c) The same as (a) for $\Gamma=5$. OCP values given by (3.2) are shown by broken line. (d) The same as (c) for $\Gamma=10$. (e) The same as (c) for $\Gamma=50$. (f) $H(r)/\Gamma$ for $r_s=1$ with $\Gamma=5$ (+), 10 (dots), and 50 (×). Solid line is interpolation for $\Gamma=5$.

in comparison with the values for the OCP.[13,14] In the case of the OCP, the nonideal part of the potential of the mean force is known to follow a simple scaling,[15]

$$H(r)/\Gamma=1.25-0.39r/a \tag{3.2}$$

for $0.4\lesssim r/a\lesssim 1.8$ and $4\le\Gamma\le 160$. As we see in these figures, $H(r)$ in our case is almost a linear function of distance but is slightly convex.

We have fitted quadratic functions of distance

$$H(r)/\Gamma=c_0+c_1r/a+c_2r^2/a^2 \tag{3.3}$$

for $H(r)$, as shown in Figs. 5(a)–5(e), with the coefficients given in Table III. In Fig. 5(f) we see that, for $r_s=1$ and $5\lesssim\Gamma\lesssim 50$, $H(r)/\Gamma$ can be approximately ex-

pressed by a single function, for example, by the fitting function for $\Gamma=5$. Comparing with OCP values c_0(OCP), c_1(OCP), and c_2(OCP) (=0), we find that these results are roughly expressed as $c_0 \sim c_0(\mathrm{OCP}) + 0.4 r_s$, $c_1 \sim c_1(\mathrm{OCP}) - 0.5 r_s$, and $c_2 \sim 0.15 r_s$. We note that the above short-range behavior of $H(r)$ cannot be fitted to the OCP pair-distribution function with Γ' ($<\Gamma$): Though the scaling of Γ has been successful in variational calculations[5,6] of the effect of electronic screening, it gives a term proportional to $(\Gamma-\Gamma')/r$ in $H(r)$ which is inconsistent with experimental results.

D. Structure factor

The structure factor $S(k)$ of ions defined by

$$n_i[g(r)-1]=(2\pi)^{-3}\int d\vec{k}[S(k)-1]\exp(i\vec{k}\cdot\vec{r}) \tag{3.4}$$

plays an important role in calculating the electronic-transport coefficients of these systems. We have computed the average of the right-hand side of

$$S(k)=\langle \rho_{\vec{g}}\rho_{-\vec{g}}\rangle/N_0 \tag{3.5}$$

which is equivalent to (3.4). Interpolating the values thus obtained for discrete wave numbers determined by the periodic boundary conditions, we have obtained the values of the structure factor shown in Figs. 6(a)–6(d) and Table IV for $r_s=1$. For $r_s=0.1$ and 0.01, it has not been possible to find meaningful deviations of the values of $S(k)$ from the OCP values.[5]

We see that the structure factor of our two-component plasma is roughly simulated by the structure factor of the OCP with reduced value of the parameter Γ. The behavior around $k=0$, however, significantly differs from the OCP values proportional to k^2.

TABLE IV. Ionic structure factor for $r_s=1$.

ka	$\Gamma=1$	$\Gamma=2$	$\Gamma=5$	$\Gamma=10$
0.8			0.20	0.12
1.0	0.57	0.41	0.23	0.14
1.4	0.64	0.48	0.30	0.20
1.8	0.70	0.56	0.38	0.28
2.2	0.77	0.66	0.49	0.37
2.6	0.82	0.74	0.62	0.50
3.0	0.86	0.81	0.75	0.65
3.4	0.89	0.86	0.84	0.82
3.8	0.91	0.90	0.90	0.94
4.2	0.94	0.94	0.96	1.02
4.6	0.96	0.96	0.99	1.06
5.0	0.97	0.98	1.00	1.07
5.4	0.98	0.99	1.01	1.06
5.8	0.99	0.99	1.02	1.04
6.2	0.99	1.00	1.03	1.02
6.6	1.00	1.00	1.03	1.01
7.0	1.00		1.02	1.00
7.4			1.01	0.99
7.8			1.00	0.99
8.2			0.99	0.99
8.6			0.99	1.00
9.0			1.00	1.00
9.4			1.00	1.00

The long-range behavior of the structure factor is related to the compressibility of the system. As is shown in the Appendix, the structure factor of ions for our model of two-component plasmas in the long-wavelength limit is given by

$$S(k)=[(k_D/k)^2/\epsilon_e(k,\omega=0)+(\partial P/\partial n_i)_T/k_BT]^{-1}\,. \tag{3.6}$$

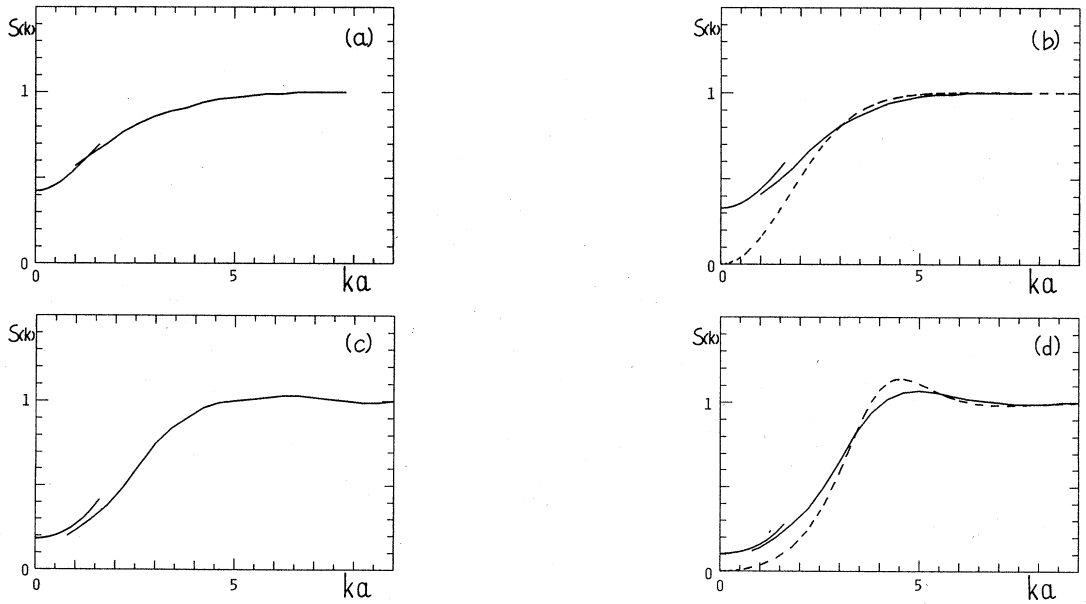

FIG. 6. (a) Ionic structure factor for $r_s=1$ and $\Gamma=1$. Solid line starting from $ka=0$ is the long-wavelength limit given by (3.6). (b) The same as (a) for $r_s=1$ and $\Gamma=2$. Broken line is OCP values (Ref. 5). (c) The same as (a) for $r_s=1$ and $\Gamma=5$. (d) The same as (b) for $r_s=1$ and $\Gamma=10$.

Here $k_D=(4\pi n_i e^2/k_B T)^{1/2}$ is the Debye wave number,

$$P=n_i k_B T+\Delta P\ , \tag{3.7}$$

and $(\partial n_i/\partial P)_T/n_i$ is the isothermal compressibility of the ion system. Thus the structure factor becomes finite at $k=0$ due to screening by electrons.

The values of (3.6) are also shown in Figs. 6(a)–6(d) and we see that experimental results are consistent with these values. The isothermal compressibility has been obtained by differentiating an expression which interpolates the values of P for $1\le\Gamma\le 50$.

IV. CONCLUSION

We have investigated thermodynamic properties of two-component plasmas, the mixture of classical ions and completely or partially degenerate electrons, in comparison with those of one-component plasmas. It has been found that the pressure of an ionic system is substantially affected by the incompleteness of degeneracy. We have computed the potential of mean force and obtained an approximate scaling for $H(r)$. The structure factor of ions has also been obtained and is shown to be consistent with the long-wavelength behavior determined by the compressibility.

ACKNOWLEDGMENTS

The authors would like to thank Professor S. Ichimaru for discussions on preliminary results. Thanks are also due to Professor Y. Furutani for his interest in the work and Dr. A. Fukuyama for graphic software. Numerical computations have been done at the Okayama University Computer Center, the Institute of Plasma Physics of Nagoya University, and the Computer Center of the University of Tokyo. This work has been partially supported by Grants-in-Aid for Scientific Researches of the Ministry of Education, Science, and Culture of Japan Nos. 56460183 and 57340023.

APPENDIX

When we introduce into our system the static external-ion density

$$\delta\rho^{\rm ext}_{\vec{k}}\exp(i\vec{k}\cdot\vec{r})\ , \tag{A1}$$

the force (per unit volume) experienced by ions is given by

$$-i\vec{k}[4\pi e^2/k^2\epsilon_e(k,0)]\delta\rho^{\rm ext}_{\vec{k}}\exp(i\vec{k}\cdot\vec{r})\ . \tag{A2}$$

Here $\epsilon_e(k,0)$ is the static dielectric response function of electrons and we implicitly take the real part of all quantities. For long wavelengths, this force is balanced by the pressure gradient as

$$-[(k_D/k)^2/\epsilon_e(k,0)]\delta\rho^{\rm ext}_{\vec{k}}=[(\partial P/\partial n_i)_T/T]\delta\rho_{\vec{k}}\ , \tag{A3}$$

where P is given by (3.7) and $\delta\rho_{\vec{k}}$ is the induced density of ions.

We note that the pressure of ion system P is defined as the volume derivative of the Helmholtz free energy with the charge neutrality condition satisfied throughout the change of the volume. Thus the induced ion density in (A3) is related to the external charge density (A1) by

$$\delta\rho_{\vec{k}}=\{[\epsilon(k,\omega=0)]^{-1}-1\}(\delta\rho^{\rm ext}_{\vec{k}}-\delta\rho_{\vec{k}})\ , \tag{A4}$$

where $\epsilon(k,\omega=0)$ is the static dielectric response function of the *ion* system. The second term on the right-hand side is the compensating background charge density which is added in order to maintain the charge neutrality; both $\delta\rho^{\rm ext}_{\vec{k}}$ and this compensating background charge density work as the source of the external field $(\delta\rho^{\rm ext}_{\vec{k}}-\delta\rho_{\vec{k}})$ to the ion system.

The structure factor of ions is related to the static dielectric response function of the ion system by the fluctuation-dissipation theorem. Since the interaction potential between ion density and external ion density is $4\pi e^2/k^2\epsilon_e(k,0)$ in our case, the fluctuation-dissipation theorem now reads

$$S(k)=(k/k_D)^2\epsilon_e(k,0)\{1-[\epsilon(k,\omega=0)]^{-1}\}\ . \tag{A5}$$

Combining this relation with (A3) and (A4), we have (3.6). It should be noted that (3.6) gives the long-wavelength behavior of the structure factor in the system of ions described by the model Hamiltonian (2.6) and is therefore different from the compressibility sum rule of the two-component system.[16] Setting $\epsilon_e(k,0)=1$ in (3.6), we have the known result for the OCP which has been obtained[17] by another method.

[1]M. Baus and J. P. Hansen, Phys. Rep. **59**, 1 (1980); S. Ichimaru, Rev. Mod. Phys. **54**, 1017 (1982).
[2]W. B. Hubbard and W. L. Slattery, Astrophys. J. **168**, 131 (1971).
[3]W. B. Hubbard, Astrophys. J. **176**, 525 (1972).
[4]H. E. DeWitt and W. B. Hubbard, Astrophys. J. **205**, 295 (1976).
[5]S. Galam and J. P. Hansen, Phys. Rev. A **14**, 816 (1976).
[6]H. Iyetomi, K. Utsumi, and S. Ichimaru, J. Phys. Soc. Jpn. **50**, 3769 (1981).
[7]J. Lindhard, K. Dan. Vidensk. Selsk. Mat. Fys. Medd. **28**, No. 8 (1954).
[8]J. Hubbard, Proc. R. Soc. London, Ser. A **243**, 336 (1957).
[9]S. Ichimaru and K. Utsumi, Phys. Rev. B **24**, 7385 (1981).
[10]B. Jancovici, Nuovo Cimento **25**, 428 (1962).
[11]N. Metropolis, A. W. Rosenbluth, M. N. Rosenbluth, A. H. Teller, and E. Teller, J. Chem. Phys. **21**, 1087 (1953).
[12]W. L. Slattery, G. D. Doolen, and H. E. DeWitt, Phys. Rev. A **26**, 2255 (1982).
[13]S. G. Brush, H. L. Sahlin, and E. Teller, J. Chem. Phys. **45**, 2102 (1966).
[14]J. P. Hansen, Phys. Rev. A **8**, 3096 (1973).
[15]H. E. DeWitt, H. C. Graboske, and M. S. Cooper, Astrophys. J. **181**, 439 (1973); N. Itoh, H. Totsuji, and S. Ichimaru, *ibid.* **218**, 477 (1978).
[16]M. Watabe and M. Hasegawa, in *The Properties of Liquid Metals* (Proceedings of the Second International Conference, Tokyo, 1972), edited by S. Takeuchi (Taylor and Francis, London, 1973), p. 113.
[17]P. Vieillefosse and J. P. Hansen, Phys. Rev. A **12**, 1106 (1975).